Electronic Background Rejection in a New Ultra-Low Background Alpha Particle Counter

W. K. Warburton and B. Dwyer-McNally
XIA LLC, 8450 Central Ave, Newark, CA 94560

Abstract:

Low background alpha-particle (α) counting is required in the semiconductor industry, where α's produce single event errors. Industry roadmaps call for measuring α emissivities at 0.0005 α/cm^2-hr, while current commercial counter backgrounds are 0.005 α/cm^2-hr, a factor of 10 too high. This paper shows that, by designing an ionization chamber so that ionization tracks collected from the sample have long risetimes while those collected from the anode have short risetimes, signal risetime analysis can distinguish α emanation location within the counter. Coupled with a guard electrode to reject tracks emitted from the counter sidewalls, the method can achieve backgrounds approaching 0.0001 α/cm^2-hr, a factor of 20 lower.

PACS code: 29.40.Cs and 29.40.Gx

Keywords: alpha-particle counter, low background

Corresponding Author:

Dr. William K. Warburton
XIA LLC
8450 Central Avenue
Newark, CA 94560-3430 USA
Tel: 1-510-494-9020 x12; Fax: 1-510-494-9040
e-mail: bill@xia.com

I. Introduction

The ability to measure materials' α emissivity (in α/cm^2-hr) is critical to the semiconductor industry for controlling levels of alpha emitters in packaging materials, since alpha particles can change the logic state of electronic circuits, a source of considerable concern. The SEMATECH consortium has issued an industry roadmap projecting a need for materials emitting fewer than 0.0005 α/cm^2-hr, [1] which is a problem, since the best available commercial instrument, a gas filled proportional counter, [2] is limited to 0.005 α/cm^2-hr by its inherent radioactivity. In this paper we describe an approach that presently, is approaching background levels of 0.0001 α/cm^2-hr, which is 20 times lower. [3]

II. The importance of low backgrounds

A simple example shows why low counter background is critical to successfully counting low-emissivity samples. We place a sample producing S counts/hr into a counter with a background rate of B counts/hr and ask for the time t to measure S with 99% reliability. Since the detected rate is R = S + B, we find S from:

$$St = Rt - Bt \pm \left[Rt + Bt\right]^{0.5} . \tag{1}$$

Setting the measured counts to K times their standard deviation and replacing R by S+B in the error term, we find the required counting time t:

$$t = \frac{K^2}{S^2}\left(S + 2B\right), \tag{2}$$

which scales as S^{-1} when B is small compared to S and as S^{-2} when B is large compared to S.

We examine two cases. The first, the commercial machine, has a 1,000 cm^2 sample and a background rate of 0.005 α/cm^2/hour (B = 5). The second, our new instrument, has an 1,800 cm^2 sample area and a background rate of 0.0001 α/cm^2/hr (B = 0.18). We measure three samples with emissivities of 0.005, 0.001, and 0.0005 α/cm^2/hr, the latter being the SEMATECH milestone. To achieve a 99% reliable measurement, so that our measured value will reflect the sample plus background count distribution 99% of the time, a table of normal errors gives K = 2.33 in Eqn. 2. The resulting estimate of S will not be particularly accurate, but its primary use will be to set an upper bound on S.

Table 1 shows the resulting measurement times. The differences in counting times are striking. The standard instrument can measure at 0.005 α/cm^2/hr in a little over three hours, but takes 60 hours (2.5 days) to measure at 0.001 α/cm^2/hr and almost 10 days to reach the SEMATECH value. These times, which increase as S^{-2}, are much too long for routine screening measurements. The XIA instrument, with its much lower background, behaves quite differently, with its count times only increasing as S^{-1} and can measure at 0.0005 α/cm^2/hr in a single 8 hour shift. Because B is so low, only about 6 counts are required to determine that S is statistically greater than B.

III. The basis of the new method

The low background counter is designed to distinguish between α's emitted from the sample and α's emitted from other parts of the counter. Figure 1 shows a sketch of a typical commercial proportional counter with an anode array of fine wires at high voltage to provide gain. It shows the various sources of background α_c particles within the counter as well as the entrance of sample α_s particles through the counter's window. Within the counting chamber, all these α's create ionization tracks approximately 4 cm long, whose electrons drift to the anode wires where they are amplified and then integrated by the preamplifier. The proportional gain, which occurs locally at the anode wires, improves signal to noise ratios, but makes all signals essentially identical, as shown in Figure 2, destroying any information about the source of the initiating α.

Our new low background counter is designed as an ionization chamber, per Figure 3. The anode is now a continuous plate, surrounded by a guard electrode, the sample lies within the chamber, and the applied voltage is sufficiently low to preclude amplification. The large area sample covers the bottom surface of the counter, leaving only two major sources of background α's, the anode and the sidewalls. In this geometry, signals are generated in the anode-preamplifier circuit by charge induction. [4] Thus currents flow through, and are integrated by, the external preamplifier circuit only so long as charges (electrons primarily) are drifting within the chamber. We can therefore deduce that: 1) the integrating preamplifier's signal risetime will also exactly match the drift time; and, 2) the further the charges drift, the larger the output signal will be because of the longer integration time. By extension, α tracks coming from the sample will produce larger signals with longer risetimes than α tracks coming from the anode. Figure 4 illustrates the effect, presenting traces captured from a 200 α/s ^{230}Th source placed on the sample and anode respectively. The 30 μs sample signal risetime matches the time for electrons to drift across the 20 cm, boiloff N_2 filled counter chamber under 1,000 V bias. The anode signal risetime is much shorter because the drift length is limited to 4 cm, the ionization track length. As predicted, anode signals are much smaller than sample signals. Signals from α's emitted from the sidewalls can clearly vary between the extremes set by the sample and anode signals. However, by placing a guard electrode to always capture charge from these events, as shown in Figure 3, we can create a guard signal to identify and reject these signals. The net result is that, while ionization chamber signals have poorer signal to noise than proportional counter signals, they retain critical track origination information that can be used to eliminate background counts.

IV. Pulse shape analysis and results

We developed a computer program that automatically analyzed captured signal traces to identify the surface from which the associated α emanated by determining the amplitude and risetime of each trace. Each trace was fit using three straight lines: two horizontal lines of (typically) 40 μs duration and a third line joining them. There were only four adjustable parameters: the value and ending time of the first horizontal line and the value and starting time of the second horizontal line (i.e. the joints between the three segments). In a fit, the joint values were adjusted to minimize the t^2 deviation between the trace and the trial function. t^2, the variance divided by (N-4), was used because the number of points N being fitted varied with the time separation between the joints.

Figure 5 shows anode signal risetime versus anode signal amplitude for 10,000 points collected from each of three α source locations: centered on the sample area, centered on the anode, and centered on one sidewall. The sample results generally group about risetime 30 μs and amplitude 1000 ADC steps, while the anode results cluster about risetime 8 μs and amplitude 200 ADC steps. Sidewall events lie in the region between these two extremes, as expected. Figure 6 replots the same points showing anode signal risetime versus guard signal amplitude. Both the anode and sample events now cluster about zero ADC steps, with their widths reflecting signal noise. The sidewall events now have finite guard amplitudes, however, and can mostly be removed by a cut at 190 ACD units, which does not remove any sample events. Figure 7 repeats Figure 5 after also applying a 22 μs anode signal risetime cut to the sidewall events. Only 7 of the original 10,000 sidewall events survive with anode amplitudes greater than 250. The latter cut on anode energy is used to remove anode "noise" events – the anode signals with amplitudes about 100 ADC steps and risetimes ranging from 12 to 46 μs. Combined with the 22 μs anode risetime cut, only 21 of the original 10,000 anode source traces survive. At least 12 of these are almost certainly real α events coming from the empty sample tray itself, which was not a particularly low background material. Given a 50 sec collection time (10,000 counts/200 counts/sec) and an 1,800 cm^2 tray area, this implies a sample tray α emissivity of 0.5 $\alpha/cm^2/hr$,.which could easily arise just from exposure to Radon in the air.

Figure 8 shows a more careful sample measurement: a mirror surface stainless steel sample tray that was cleaned with a dilute HCl solution, rinsed in distilled water and alcohol, and transferred under N_2 to our counter, which was purged with boiloff N_2 for 30 minutes before counting commenced. Total tray exposure to air was probably less than 2 minutes. Under these conditions, stainless steel was a relatively low background material, giving only 21 α's in 8 hours, for an emissivity of 0.0015 $\alpha/cm^2/hr$. The three counts with risetimes about 25 μs and amplitudes of 400 may be noise or other background events, leading to a background estimate of 0.0002 $a/cm^2/hr$, which is very close to our goal of 0.0001 $\alpha/cm^2/hr$. The events that lie in the excluded region of risetimes less that 22 μs and amplitudes greater than 250 ADC units are currently unexplained since, theoretically, they cannot be generated by α's emanating from any counter or sample surface. We are currently investigating such possibilities as rare capacitor breakdown discharges and nitrogen gas fragmentation induced by cosmic ray generated high energy neutrons. Understanding and eliminating this class of possible background events will help us achieve our next goal of 0.00001 $\alpha/cm^2/hr$ background rates.

V. Conclusions

By designing a counter whose signals retain α ionization track point of emanation information, we could apply signal shape analysis to identify those points of emanation and so eliminate non-sample background counts. This approach achieved backgrounds nearly at the 0.0001 $\alpha/cm^2/hr$ level, which is critical to measuring materials at the 0.0005 $\alpha/cm^2/hr$ SEMATECH guideline level.

Acknowledgments:

This work was supported by the National Institutes of Science and Technology under SBIR Contract No. 50-DKNB-1-SB-85 and by the U.S. Department of Energy under SBIR grant number DE-FG02-04ER84120.

References:

[1] R. Baumann and E. Smith, "Call for improved ultra-low background alpha-particle emission metrology for the semiconductor industry", *Int. SEMATECH Technology Transfer* #01054118A-XFR, 2001.

[2] The Model 1950 from Spectrum Sciences, Inc. Details are available from their website: www.ssi-iico.com.

[3] W.K. Warburton, John Wahl, and Michael Momayezi, "Ultra-low background gas-filled alpha counter", *U.S. Patent 6,732,059* (Issued May 4, 2004).

[4] G.F. Knoll, *Radiation Detection and Measurement, 3rd Ed.*, (John Wiley & Sons, New York, 2000) Appendix D.

Figure Legends:

Figure 1 : Sketch of conventional proportional counter, showing counter α_c and sample α_s sources.

Figure 2: Typical preamplifier output from Fig. 1 proportional counter.

Figure 3: Sketch XIA's ion chamber counter.

Figure 4: Preamplifier signals from three source location within the XIA counter: the sample, the anode; and the sidewall.

Figure 5: Anode risetime versus anode amplitude for the three α source locations (■ = sample, ○ = sidewall, ∗ = anode).

Figure 6: Anode risetime versus guard amplitude for the same signals as Figure 5. The amplitude cut excludes sidewall events.

Figure 7: The data of Figure 5 after removing signals that failed the sidewall event cut. The risetime cut excludes anode source events.

Figure 8: Data from a cleaned stainless steel sample (■ = sample, ∗ = anode).

Tables:

#	**B** (c/h)	**S** (c/h)	**t** (h)	**N_B**	**N_R**	**N_S**
S-1	5	5	**3.3**	16	33	16±7
S-2	5	1	**59.7**	299	358	60±26
S-3	5	0.5	**228**	1140	1254	114±49
X-1	0.18	5	**0.63**	0.11	5.76	5.7±2.4
X-2	0.18	1	**3.62**	0.65	7.17	6.5±2.8
X-3	0.18	0.5	**8.44**	1.52	9.12	7.6±3.3

Table 1: Counting times and counts for two instruments (S and X) and three values of S.

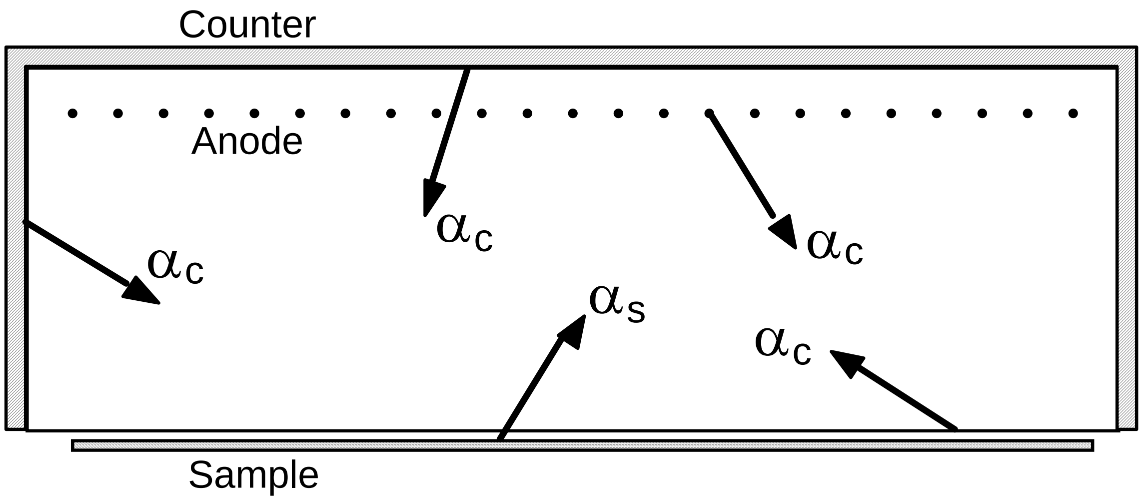

Figure 1:

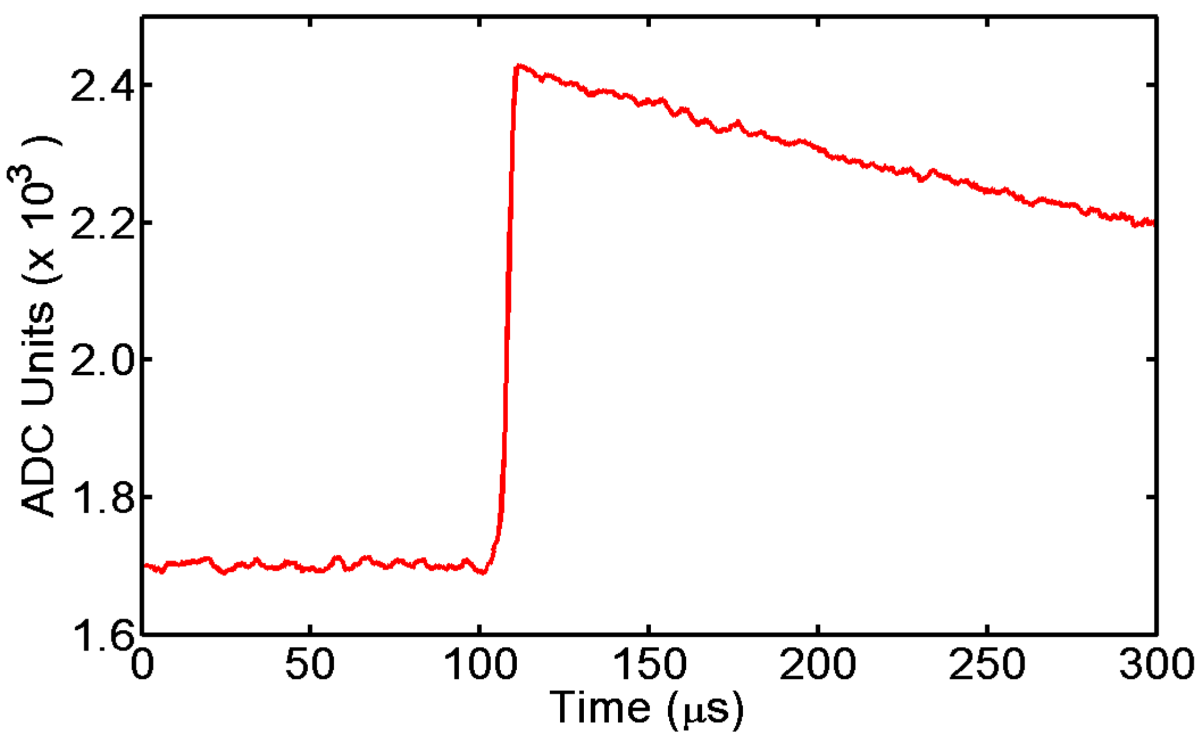

Figure 2:

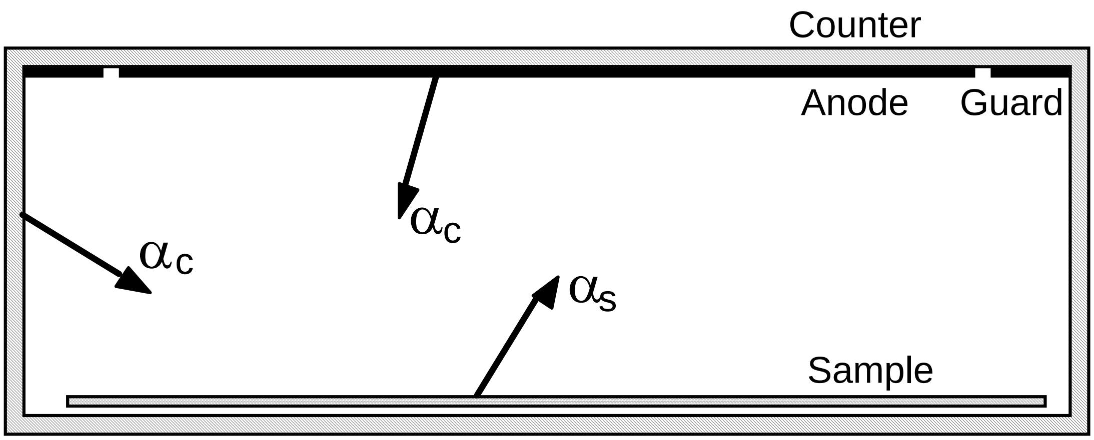

Figure 3:

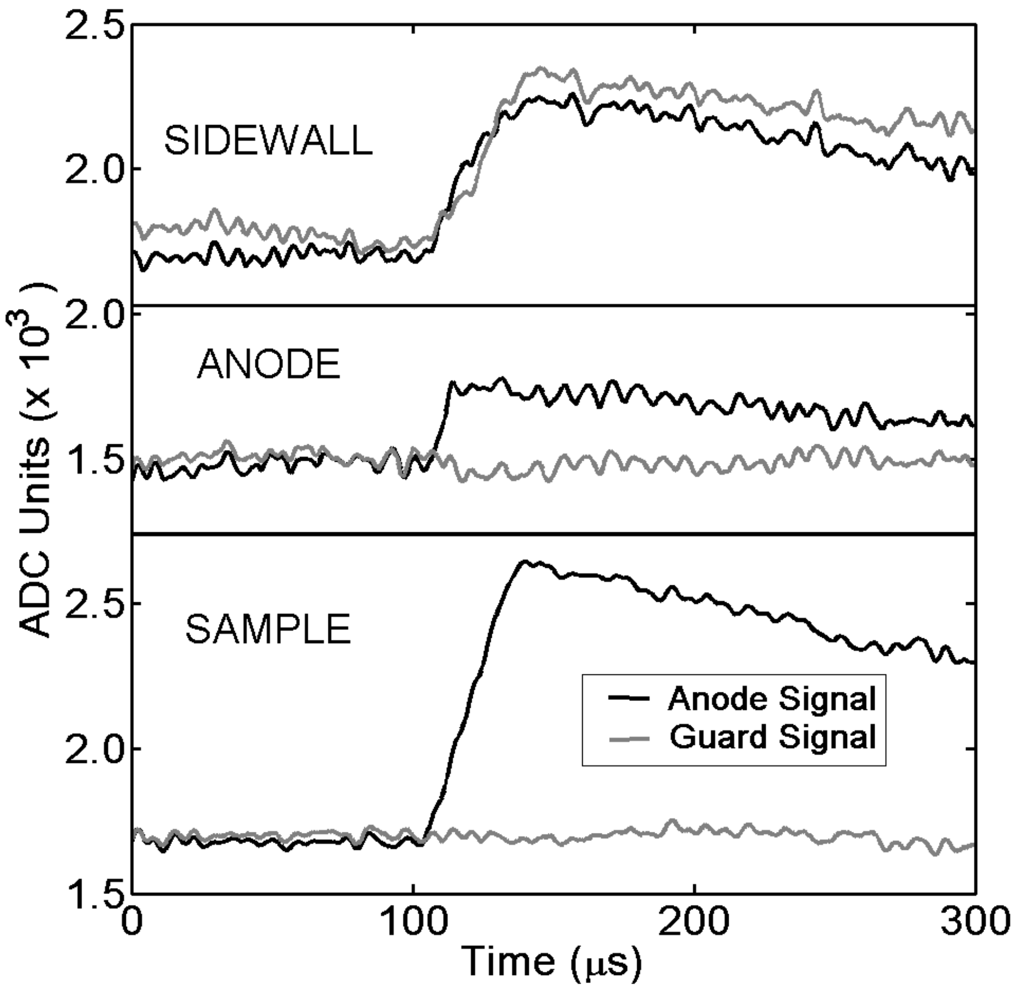

Figure 4:

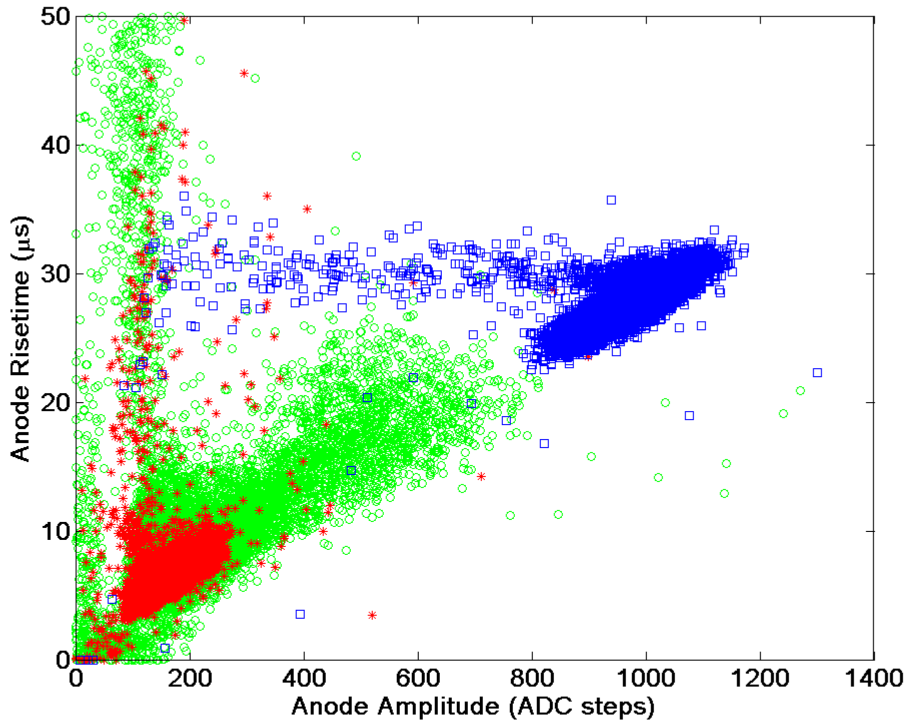

Figure 5:

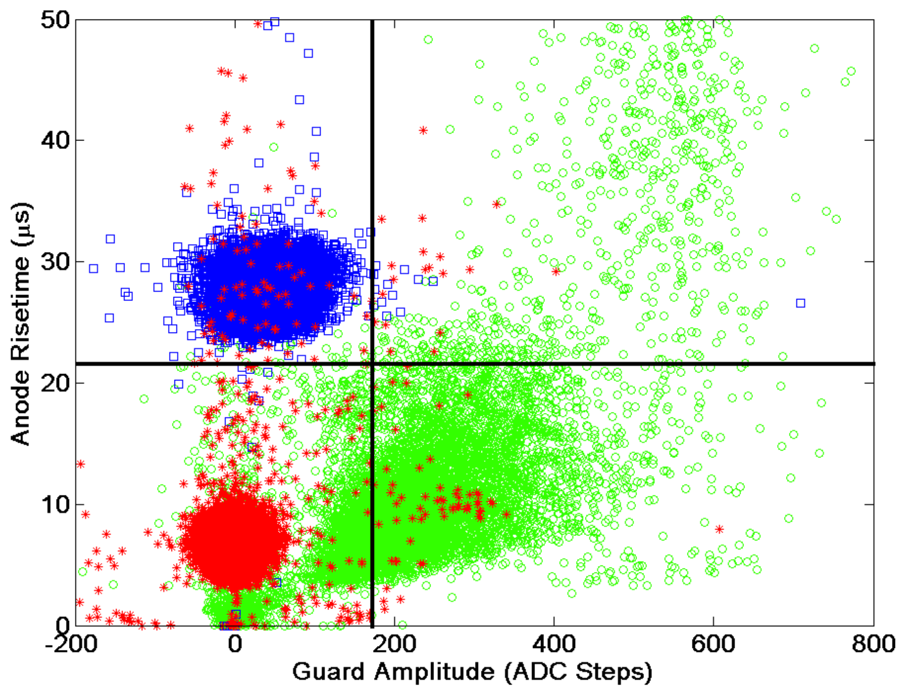

Figure 6:

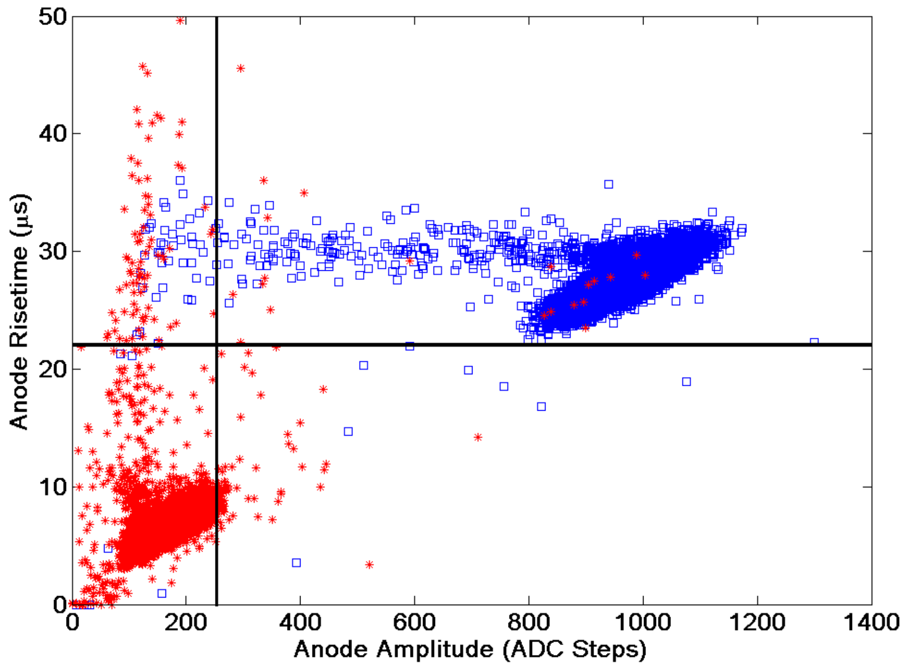

Figure 7:

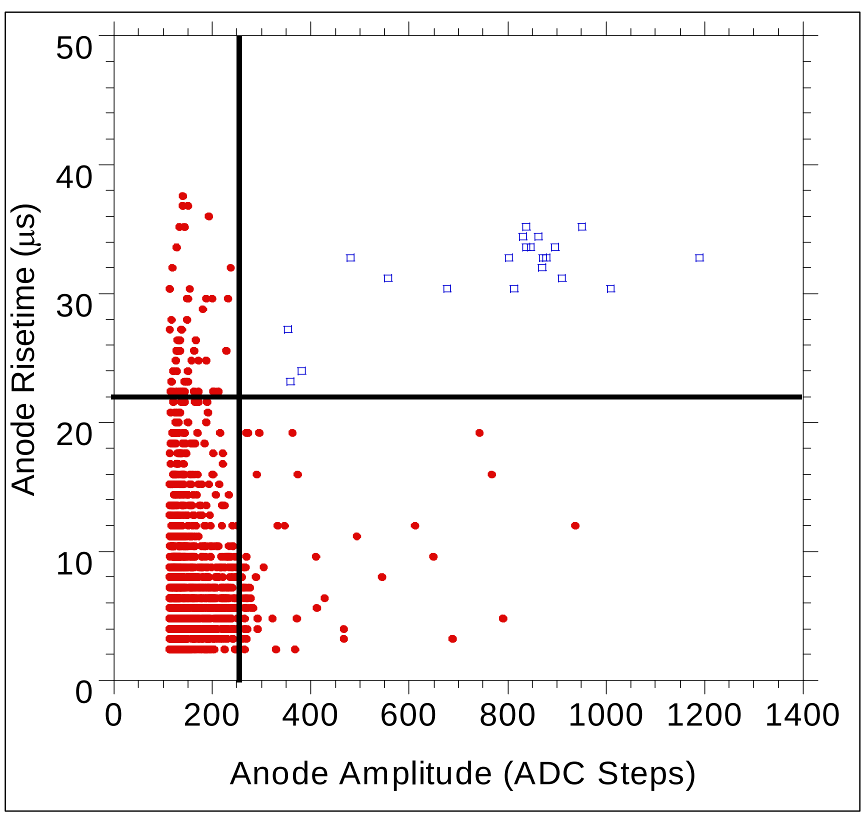

Figure 8: